

Infrared to Ultraviolet Wavelength-Dependent Variations Within the Pulse Profile Peaks of the Crab Nebula Pulsar

S.S. Eikenberry, G.G. Fazio, S.M. Ransom

Harvard-Smithsonian Center for Astrophysics, Cambridge, MA 02138

J. Middleditch

Los Alamos National Laboratory, Los Alamos, NM 87545

J.A. Kristian

Observatories of the Carnegie Institution of Washington, Pasadena, CA 91101

C.R. Pennypacker

Space Sciences Laboratory, University of California, Berkeley, CA 94720

Received _____; accepted _____

ABSTRACT

We present evidence of wavelength-dependent variations within the infrared, optical, and ultraviolet pulse profile peaks of the Crab Nebula pulsar. The leading and trailing edge half-width half-maxima of the peaks display clear differences in their wavelength dependences. In addition, phase-resolved infrared-to-ultraviolet color spectra show significant variations from the leading to trailing edges of the peaks. The color variations between the leading and trailing edges remain significant over phase differences smaller than 0.0054, corresponding to timescales of $< 180\mu\text{s}$. These results are not predicted by any current models of the pulsar emission mechanism and offer new challenges for the development of such models.

Subject headings: pulsar: individual (PSR0531+21) - instrumentation: detectors - stars: neutron

1. Introduction

Astronomers have been studying pulsars for nearly 30 years and yet, we still have no clear understanding of the emission mechanisms that produce the trademark pulsations. However, pulsar emission models do exist for some pulsars, in particular the γ -ray pulsars, of which the Crab Nebula pulsar is the most well-studied. In current models of Crab Nebula pulsar emissions, primary energy generation occurs in particle accelerator “gaps” in the outer magnetosphere (i.e. Cheng, Ho, and Ruderman 1986ab; Chiang and Romani (1994); Romani and Yadigaroglu (1995) - hereafter CHRab, CR94, and RY, respectively). The accelerated particles produce γ -rays through curvature radiation, and these γ -rays interact with the magnetosphere in a complex manner to produce the X-ray, UV, optical, and infrared pulsations, so that the non-radio emissions are closely linked to each other. Because of this linkage, we are investigating the pulsar emission mechanism through the UV, optical, and infrared emissions, where high signal-to-noise observations are more practical to obtain than in the X-ray and γ -ray wavebands (see Ransom *et al.* (1994) for earlier results).

While the emission models mentioned above vary in their underlying assumptions, they share several common features. Not least among these is the assumption that the emission arises in an essentially uniform region, with the observed shape and sharpness of the pulse profile peaks¹ (see Figure 1) resulting from a combination of time-of-flight delays and relativistic aberration of the magnetic field lines. In some of these models (CHRab), the mapping from observed pulse phase to position in the emission region is neither one-to-one nor continuous, so that the observed flux in a given pulse phase interval is a combination of emission from multiple disjoint sections of the emission region, and the

¹We refer to the 2 major features in the profile as Peak 1 and Peak 2, joined by the Bridge. This is to avoid confusion, as some previous authors refer to the Bridge as the “Interpulse”, while others use that name for Peak 2.

locations of the particular sections which contribute emission to that phase interval depend on the observer’s viewing angle. This mixing of physical regions within the observed phase interval effectively averages the emission over a range within the emission region, with the largest amount of averaging at the peak maximum. Thus, the observed emission properties should remain constant or change slowly and smoothly over the peak, and should certainly not exhibit any sharp changes near the peak maximum. It is with this prediction in mind that we examine the peaks of the Crab Nebula pulsar for wavelength-dependent variations about the peak maximum.

2. Observations and Data Reduction

We made the infrared observations for this work in the J ($1.25\mu\text{m}$), H ($1.65\mu\text{m}$), and K ($2.2\mu\text{m}$) bands using the Solid-State Photomultiplier (SSPM) instrument on the Multiple Mirror Telescope² on January 18-22, 1995. The SSPM instrument (Eikenberry, *et al.*, 1996) is a high-speed near-infrared photometer, with single-photon-counting performance and submicrosecond time resolution, based on the Solid-State Photomultiplier detector developed by the Rockwell International Science Center (Petroff, *et al.*, 1987). For these observations, we recorded counts from the SSPM using $20\mu\text{s}$ time bins, with an EG&G rubidium frequency standard for timing reference. The resulting time-series were corrected to the solar system barycenter and used to determine the pulsar timing characteristics (see Eikenberry, *et al.* (1996) for details). We determine the pulsar frequency to be $f_0 = 29.9047918 \pm 0.0000013$ Hz and the frequency derivative to be $\dot{f} = -3.83 \pm 0.12 \times 10^{-10}$ Hz/s at MJD 49736.17666605, in good agreement with the Jodrell Bank timing ephemeris

²The MMT is jointly owned and operated by the University of Arizona and the Smithsonian Astrophysical Observatory.

(A.G. Lyne, personal communication). Given this timing solution, we then create pulse profiles for the Crab Nebula pulsar in each of the J,H, and K wavebands by folding the barycentered time-series at the appropriate values of f and \dot{f} , and then background-subtracting the profiles. In order to augment these data, we also include optical (V) and UV profiles taken with the HST High-Speed Photometer (HSP) (Percival *et al.*, 1993) in the analyses.

3. Analysis

In order to study wavelength-dependent variations in the peaks of the Crab Nebula pulsar, we divide each peak into 2 halves - the leading and trailing edges - with the emission maximum marking the point of division. We illustrate the resulting phase conventions for the V-band in Figure 1. As mentioned above, we expect that the emission properties should not change sharply near the emission maximum. Therefore, the first step in the analysis is to examine the wavelength dependences of the shape about the peak maximum - in this case the half-width half-maxima of the leading and trailing edges of the peaks. Next, we analyze the color spectra of the peaks for significant variations between the leading and trailing edges. Finally, we perform analyses to reveal the range of “timescales” for the phase-resolved color variations in Peak 1.

3.1. Peak half-width half-maximum

We measure the half-width half-maximum (HWHM) by simply taking the difference in phase between the peak maximum and the points where the flux drops to 1/2 of the maximum value. While this procedure is straightforward, it does not easily allow us to determine the uncertainties in the HWHM values due to the Poisson statistics of the

pulse profiles. In order to estimate these uncertainties, we use a Monte Carlo simulation, proceeding as follows. First, we fit independent third-order polynomials to the leading and trailing edges of the peaks, and measure the HWHM from the points where the fits equal one-half of the peak maximum. (In all cases, the fit determination of the HWHM matches the manually measured HWHM.) Next, we take the phase bins in the peak region and assume that the noise in the number of counts in each bin follows a Poisson distribution. We then take the fit to the peak and add to each bin a normally-distributed random number with a variance corresponding to the Poisson noise for that bin. We fit this new profile and measure the new half-widths, and then repeat the procedure 1000 times for each peak. Finally, we take the standard deviation of the simulated half-widths to be the 1σ uncertainty in the measured value. The resulting HWHM values and uncertainties for Peak 1 are plotted in Figure 2.

The result of this analysis is that the wavelength dependences of the HWHM for the leading and trailing edges are noticeably different. The Peak 1 leading edge HWHM rises from the UV to J-band, and then shows a break at $1.25\mu\text{m}$, declining from J-band to K-band. Meanwhile, the Peak 1 trailing edge HWHM rises slowly from UV to J-band or H-band, and then sharply to K-band. While the HWHM values for Peak 2 are noisier, if we divide the Peak 2 leading edge HWHM by the trailing edge HWHM and fit the resulting ratio with a flat line, we find $\chi^2 = 61$ for 4 degrees of freedom. This indicates a significant difference between the wavelength dependences for the leading and trailing edge HWHM for Peak 2. Although previous work has shown weak evidence of similar effects (Pravdo and Serlemitsos, 1981), these data present the first significant evidence of wavelength-dependent variations within the individual peaks of the Crab Nebula pulsar.

3.2. Phase-resolved spectra

We can also investigate the presence of wavelength-dependent variations through the color spectra of the peaks. The time resolution of our SSPM data and the HST HSP data allows us to construct phase-resolved spectra of the Crab Nebula pulsar. We divide the pulse profiles into phase segments, and calculate the fraction of the total photon counts received in each segment using the phase conventions shown in Figure 1. We then take these fractional photon fluxes from each waveband for a given phase segment to produce a relative color “spectrum”. Note that the normalization between bands in the relative color spectrum is essentially arbitrary. However, these relative, unnormalized color spectra are the most sensitive tools we can use to analyze color differences or similarities between different phase intervals of the pulse profile, given the large uncertainties introduced by reddening corrections to the Crab Nebula pulsar.

We present the relative color spectra for the leading and trailing edges of Peak 1 in Figure 3(a). Note that there is a distinct difference between the spectral shapes of the leading and trailing edges of the peak. Similarly, in Figure 3(b), we present the relative spectra for the leading and trailing edges of Peak 2. Again, the leading and trailing edges exhibit markedly different colors. Thus, these results confirm the presence of wavelength-dependent variations in the peaks of the Crab Nebula pulsar.

3.3. Rapid color variability with phase

We present a series of unnormalized Peak 1 color spectra with a phase resolution corresponding to 1 ms in Figure 4. Note that the spectral shape changes as a function of phase on the 1 ms timescale of the frames. Furthermore, the difference in spectral shape between the Peak 1 leading and trailing edges (see Figure 3) appears clearly even in the

two 1-ms frames bracketing the peak maximum (phase = 0).

In order to determine the minimum phase difference for which this color variation is resolvable, we perform the following analysis. First, for a given phase interval, we calculate the fractional photon flux before and after the peak maximum in each waveband. We then divide the leading edge photon fluxes by the trailing edge photon fluxes, resulting in values which should all be equal (within errors) for the case of no leading/trailing color variation, and we calculate χ^2 for the variation of this ratio from a flat line. We must also take into account the uncertainties in the peak location and do so by repeating the procedure for all possible combinations of the Peak 1 location in the 5 pulse profiles (within 1σ uncertainties). We then take the minimum χ^2 value from these combinations as the limiting case for the significance of color variability over the phase interval in question, and we repeat this analysis over a range of phase intervals down to $20\mu\text{s}$. The shortest phase interval which shows significant variations at the 99.9% level is 0.0054, corresponding to a time of $180\mu\text{s}$. Thus we conclude that the minimum “timescale” for color variations with phase within Peak 1 is $< 180\mu\text{s}$.

4. Discussion

The above observations and analyses reveal significant evidence of wavelength-dependent variations within the peaks of the Crab Nebula pulsar’s pulse profile. The difference in the wavelength dependence between the leading and trailing edge HWHM of Peak 1 (Figure 2) establishes the existence of such variations for the first time. In order to exhibit such behavior, the emission process must somehow change around the peak maximum. The phase-resolved color spectra only strengthen this conclusion, exhibiting variability on timescales from milliseconds to $< 180\mu\text{s}$, with clear differences between the leading and trailing edges.

The presence of wavelength-dependent variations within the profile peaks presents some interesting questions regarding the origin of the pulse shape. As mentioned above, in current models the shape of the Crab Nebula pulsar peaks is determined by time-of-flight delays and relativistic aberration of the magnetic field lines. The observed sharp cusp of the peak maximum results from the simultaneous arrival of flux from many (possibly disjoint) physical locations within the emission region. For those models in which the observed emission in the peak maximum emanates from such disjoint physical regions (CHRab), the emission properties should not change sharply near this phase interval. While it is possible that other models (CR94, RY95) may allow such sharp variations near the maximum of Peak 1 in particular, as the mapping there from the physical emission region to the observed pulse phase may be more nearly monotonic, these models do not currently predict such variations.

We can further quantify the characteristics of the variations using the fact that the Peak 1 color spectrum varies on timescales at least as rapidly as $180\mu\text{s}$. We believe both from models (CHRab, CR94, RY95) and observations (Smith *et al.*, 1988) that the Crab Nebula pulsar's high-energy emissions originate near the light cylinder, where the magnetospheric corotation velocity approaches the speed of light. Thus, we conclude that the typical coherence length for the emission region is similar to or less than $1.8 \times 10^{-4}\text{s} \times c = 54 \text{ km}$.

5. Conclusions

We have presented evidence of wavelength-dependent variations within the pulse profile peaks of the Crab Nebula pulsar. This evidence includes differences in the wavelength dependences of the leading and trailing edge peak HWHM and color differences on timescales from milliseconds to $< 180\mu\text{s}$. This type of variation is not predicted by current pulsar emission theories, and offers new challenges for the development of such theories.

We would like to thank K. Hays, M. Stapelbroek, and R. Florence of the Rockwell International Science Center for providing the SSPM detectors and invaluable advice and support; J. Dolan and the HST HSP team for providing the optical and UV profiles; J. Geary, P. Crawford, C. Hughes of the CfA for help in constructing the SSPM instrument; D. Paolucci of the MIT Laser Spectroscopy Lab for help with the laser alignment; W. Riley of EG&G for providing the rubidium frequency standard; R. Lucinio of Caltech for maintaining the Wizards; the MMTO support crew for their assistance and donation of engineering time; A.G. Lyne of Jodrell Bank for supplying the Jodrell Bank pulsar ephemeris before publication; and R. Narayan, J. Grindlay, and F. Seward of the CfA and T.N. Rengarajan of the Tata Institute for Fundamental Research for their helpful discussions of this work. S. Eikenberry is supported by a NASA Graduate Student Researchers Program grant through Ames Research Center.

REFERENCES

Cheng, K.S., Ho C., and Ruderman, M. 1986a, *ApJ*, 300, 500

Cheng, K.S., Ho C., and Ruderman, M. 1986b, *ApJ*, 300, 500

Chiang, J. and Romani, R.W. 1994, *ApJ*, 436, 754

Eikenberry, S.S., Fazio, G.G. and Ransom, S.M. 1996, *PASP*, in press

Eikenberry, S.S., Fazio, G.G., Ransom, S.M., Middleditch, J., Kristian, J., Pennypacker, C.R., 1996, in preparation

Percival, J.W., Biggs, J.D., Dolan, J.F., Robinson, E.L., Taylor, M.J., Bless, R.C., Elliot, J.L., Nelson, M.J., Ramseyer, T.F., van Citters, G.W. 1993, *ApJ*, 407, 276

Petroff, M.D., Stapelbroek, M.G., and Kleinhans, W.A. 1987, *Appl. Phys. Lett.*, 51, 406

Pravdo, S.H. and Serlemitsos, P.J. 1981, *ApJ*, 246, 484

Ransom, S.M., Fazio, G.G., Eikenberry, S.S., Middleditch, J., Kristian, J.A., Pennypacker, C.R. and Hays, K.M. 1994, *ApJ*, 431, L43

Romani, R.W. and Yadigaroglu, I.-A. 1995, *ApJ*, 438, 314

Smith, F.G., Jones, D.H.P., Disck, J.S.B. and Pike, C.D. 1988, *MNRAS*, 233, 305.

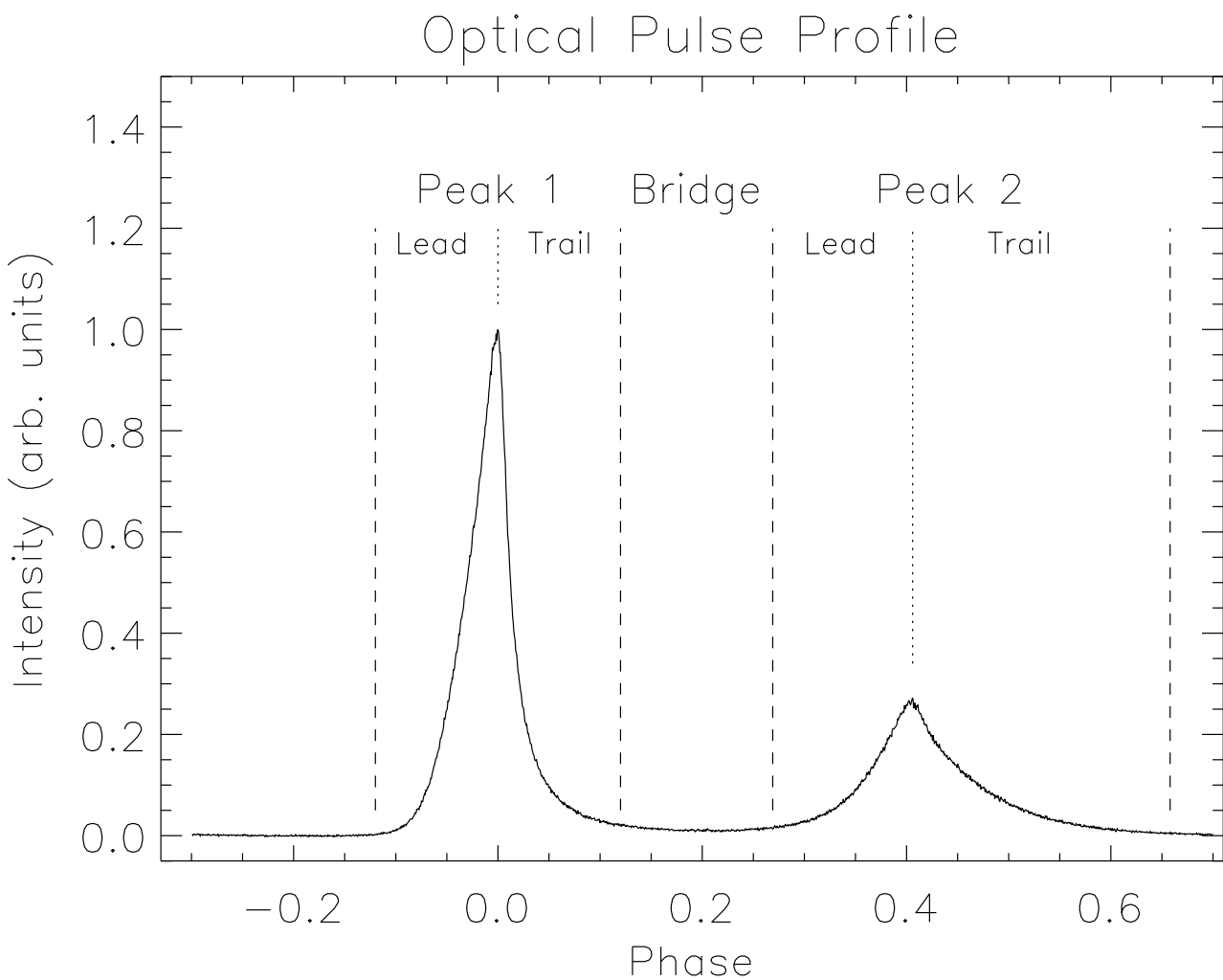


Fig. 1.— Pulse profile with phase conventions used in the analyses

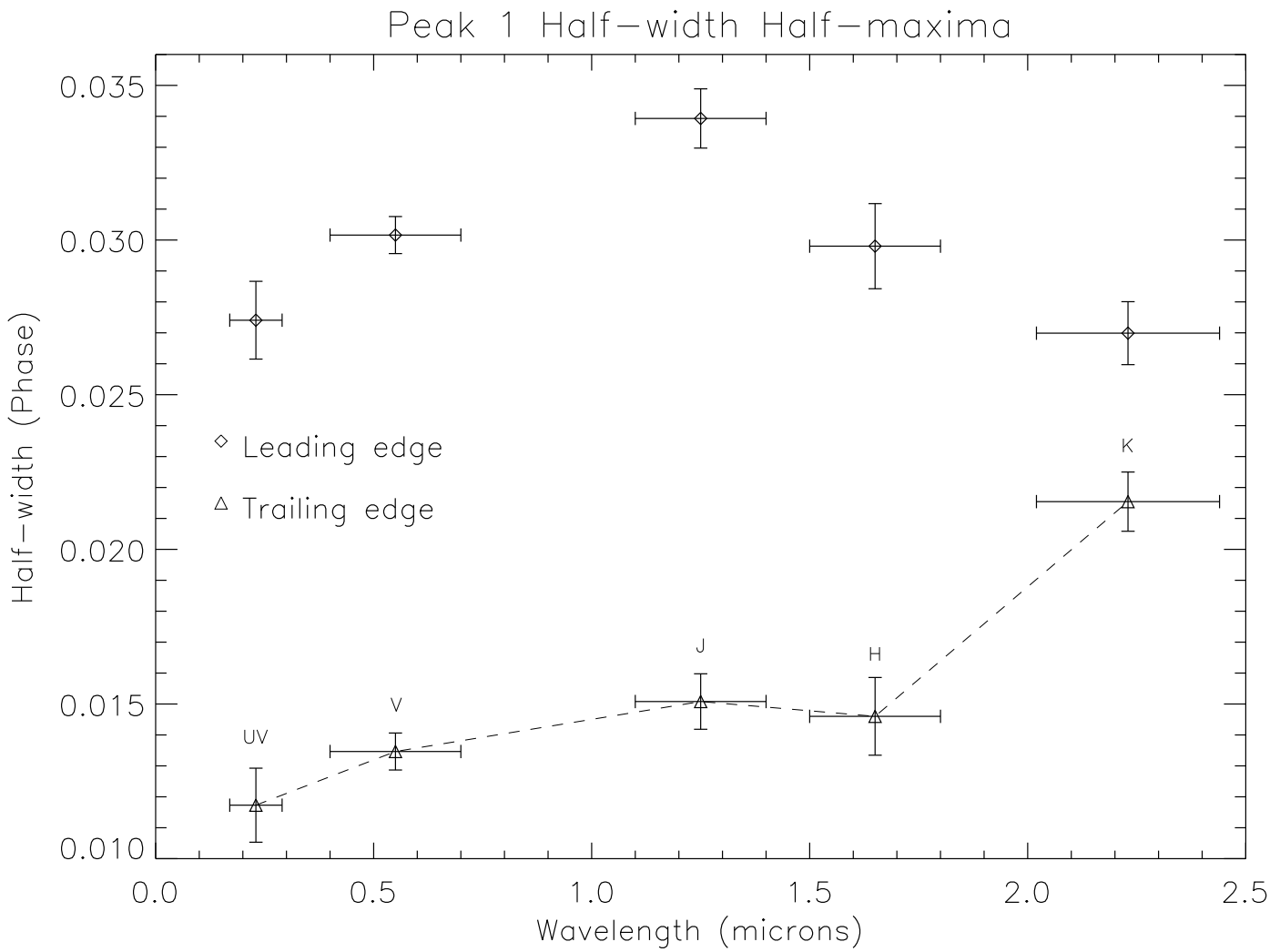


Fig. 2.— Peak half-width half-maximum versus wavelength for Peak 1 leading and trailing edges

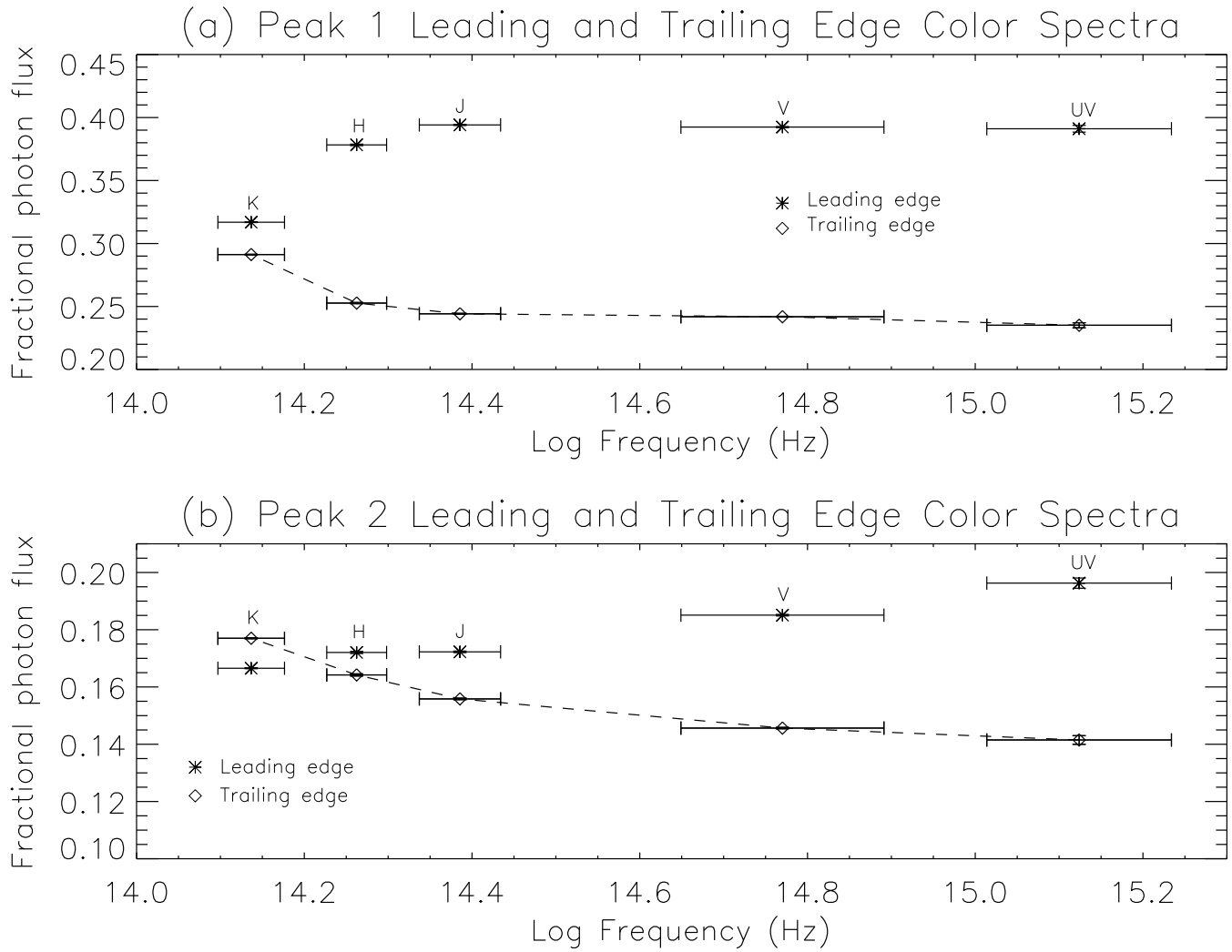


Fig. 3.— Fractional photon flux versus frequency for leading and trailing edges of (a) Peak 1, (b) Peak 2

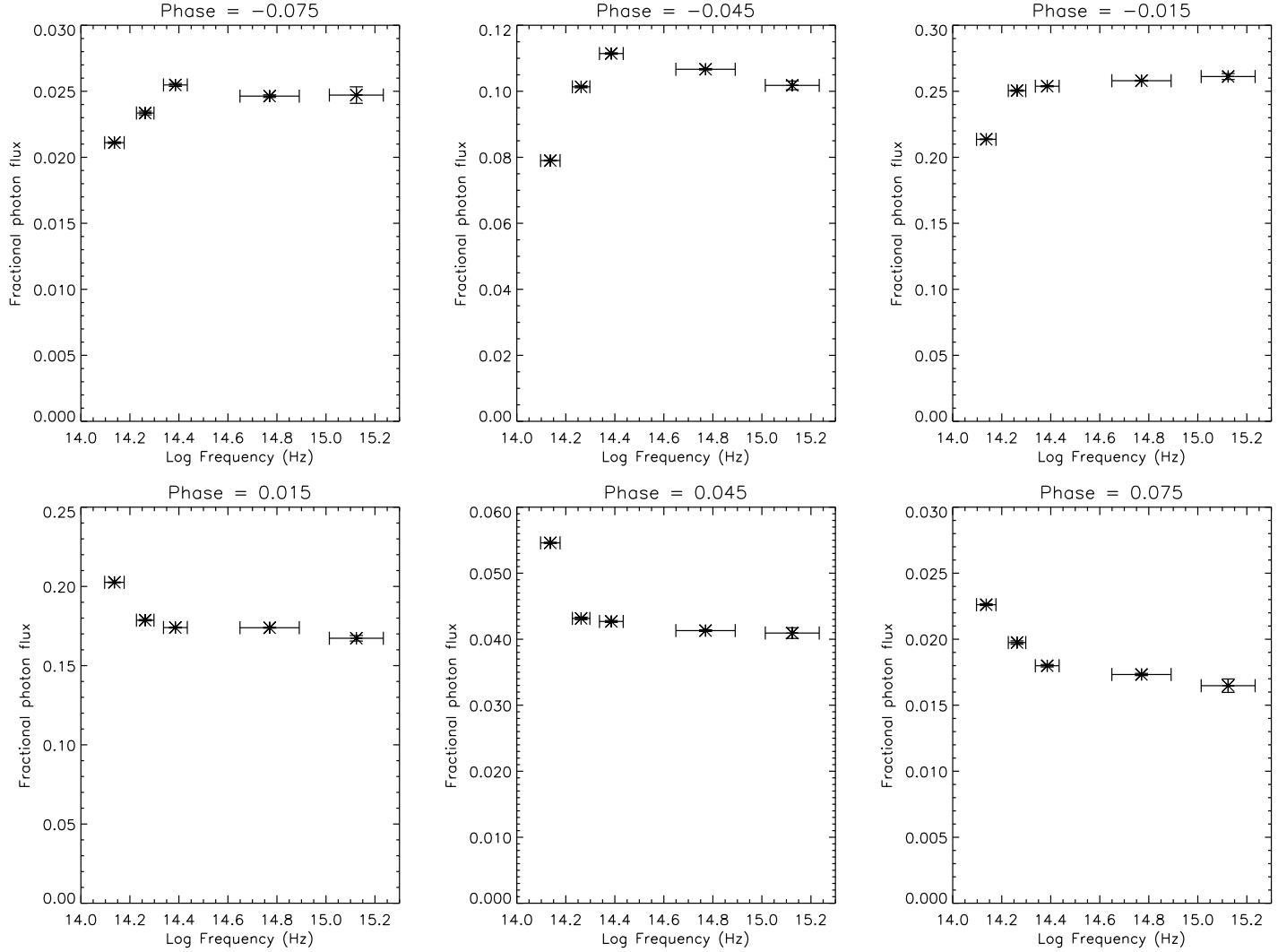


Fig. 4.— Series of phase-resolved, unnormalized Peak 1 color spectra. The phase difference from frame to frame corresponds to ~ 1 ms. Note the sharp change in spectral shape near phase=0.